OPTICAL CHARACTERISTICS AND FORMATION PROCESSES OF AEROSOLS PRODUCED BY AN OZONE AND 1-BUTENE REACTION IN OXYGEN

L. C. LEE, R. L. DAY and MASAKO SUTO

Department of Electrical and Computer Engineering, San Diego State University, San Diego, CA 92182 (U.S.A.)

(Received November 4, 1983; in revised form January 9, 1984)

Summary

Emissions from UV excitations of aerosols produced by an O_3 and 1-butene (1-C_4H_8) reaction in a flow tube were investigated. Excimer lasers and various microwave discharge lamps were used as light sources. Emissions from aerosols excited by excimer laser photons were dispersed. The emission spectrum shows molecular structure. The emission intensity is closely correlated with the aerosol scattering intensity, indicating that the emission is produced from the optical excitation of aerosols. The excitation functions for producing the aerosol scattering and emission light were investigated at various excitation wavelengths, O_3 and 1-C_4H_8 concentrations and reaction times. The aerosol formation process is speculated in accord with the data of aerosol scattering and emission light intensities. It is suggested that aerosols may be produced by two major processes: one by active chemical species initially produced from ozonolysis of 1-C_4H_8 and the other by less active species or secondary reaction products.

1. Introduction

The aerosol formation from ozone (O_3) and olefin reactions has been observed by several investigators [1 - 5]. Aerosols were formed by mixing the reactants. The relative aerosol abundance was once crudely estimated by a visual observation of the cloudiness in the gas reaction cell [1].

The optical characteristics of aerosols produced from O_3 and 1-butene (1-C_4H_8) are reported here. The aerosols were produced by gas reactions in a flow tube and then excited by UV photons. Both the optical emission spectra and the excitation spectra of aerosols by UV irradiation are investigated.

The optical data obtained are useful for understanding the aerosol formation process. It is suggested that O_3 attacks the double bond of olefins to form molozonides. The molozonides then split into small products by the

0047-2670/84/$3.00

Criegee mechanism [6] or transform into biradical intermediates by various hydrogen abstraction paths as proposed by O'Neal and Blumstein [7]. The intermediates may later break into small products or react among themselves to form embryos which may grow into aerosol particles. The aerosol formation process is speculated here using the optical data obtained.

The aerosols produced from the O_3 and olefin reactions are the important sources for the formation of photochemical smog [8 - 10]. The optical data obtained are useful for characterizing this class of aerosols. The UV scattering could be used as a way to measure the particle sizes that are typically in the range of a few hundred ångströms in the early aerosol formation stage. These small-size aerosols are not detectable by visible and IR light scattering. Optical detection has the advantages of fast response and of being non-intrusive to gas media, so it can detect aerosols *in situ* in various environments.

2. Experimental details

The experimental set-up is shown in Fig. 1. The O_3 and 1-C_4H_8 react in a flow tube which is a poly(vinyl chloride) pipe of 5 cm inside diameter (ID) and 100 cm long. The reaction products are excited in a gas cell which is a six-way stainless steel cross of 12.5 cm ID. The 1-C_4H_8 is introduced into the flow tube through a stainless steel tube of 0.63 cm ID whose length inside the flow tube is adjustable.

O_3 was produced by a high voltage a.c. discharge of O_2 in an ozonizer which was made from a double-walled glass tube of 25 mm outside diameter and 2 mm spacing. The electrodes were installed outside the glass wall. The [O_3] was measured by the attenuation of a mercury light at 253.7 nm, whose intensity was monitored by a combination of a narrow band filter (253.7 ± 10 nm) and a photomultiplier tube (PMT) (EMI 9635QB). The O_2 pressure in the flow tube was kept at about 110 Torr. The excess O_3 was destroyed by a heated trap before it entered a mechanical pump. The linear flow velocity, which was measured by the ratio of the flow distance to the

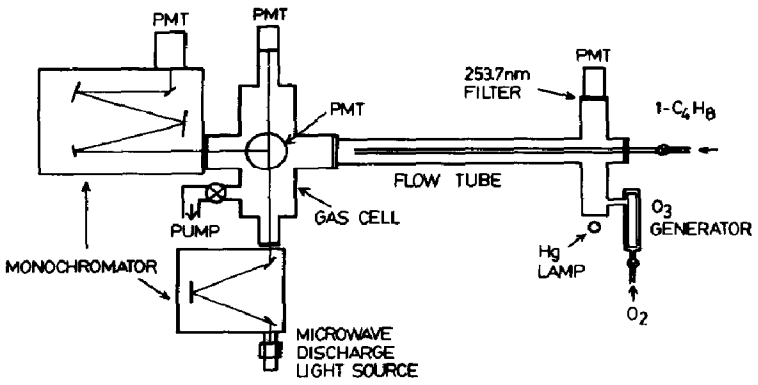

Fig. 1. Schematic diagram of the experimental apparatus (PMT, photomultiplier tube).

time interval between O_3 entering the flow tube and reaching the center of the gas cell, was kept at about 1.7 cm s^{-1}. The O_2 flow rate determined from the flow velocity was 4.0 cm^3 s^{-1} at standard temperature and pressure.

O_3 reacts with the 1-C_4H_8 added downstream. The reaction time was determined from the distance between the 1-C_4H_8 inlet and the optical excitation region. The aerosols were excited by UV light at the center of the gas cell. The UV light sources were produced by ArF and KrF excimer lasers or by a microwave discharge of a trace of mercury, I_2, NO_2 or CH_4 in argon. The light source intensity was monitored with a combination of a PMT and sodium salicylate coated on a window. The sodium salicylate converts UV light into visible light with a conversion efficiency nearly constant over the 180 - 300 nm region [11, 12]. The wavelength of the microwave discharge light source was discriminated by a 0.25 m monochromator before it entered the gas cell. The emission produced from the UV excitation of aerosols was measured by a combination of a PMT and an optical filter. The emissions were observed in directions orthogonal to the excitation light source.

The emission from the excitation of aerosols by excimer laser photons (Lumonics 861S) was dispersed. The typical laser energy was 50 mJ $pulse^{-1}$ and the pulse duration was 10 ns. The laser energy was constantly monitored by a vacuum diode which was made from a copper plate and an anode biased with 90 V. The optical emission was dispersed by a 0.5 m monochromator (manufactured by Acton Inc.) and detected by a cooled PMT (EMI 9558QB). The signal was processed by a photon counting system, which was gated so that it was active only within 40 μs following the laser pulse. This gated system has two purposes: (i) to cut down the photomultiplier noise and (ii) to ensure that the emission is truly produced by laser excitation.

The chemiluminescence was observed from the O_3 and 1-C_4H_8 reaction when the [O_3] and [1-C_4H_8] were low and the reaction distance was short. The chemiluminescence intensity decreases when the [O_3] and/or the [1-C_4H_8] increased. The intensity also decreases with increasing reaction distance. We have subtracted the chemiluminescence intensity out from the optical signals observed, so the emission and scattering light intensities presented below do not include the chemiluminescence.

3. Results and discussion

3.1. Aerosol optical characteristics

3.1.1. Emission spectra

The emission spectra produced by the ArF laser excitation of the O_3 and 1-C_4H_8 reaction products are shown in Fig. 2 for the reaction distances l of 10, 40, 80 and 110 cm. The reaction distance was measured from the 1-C_4H_8 inlet to the laser interaction region. The partial pressures of O_2, O_3 and 1-C_4H_8 for all measurements shown in Fig. 2 were fixed at 114 Torr, 0.4 Torr and 0.2 Torr respectively. The monochromator resolution was set at 5 Å. The laser energies for producing the spectra of Fig. 2 were about 52 mJ

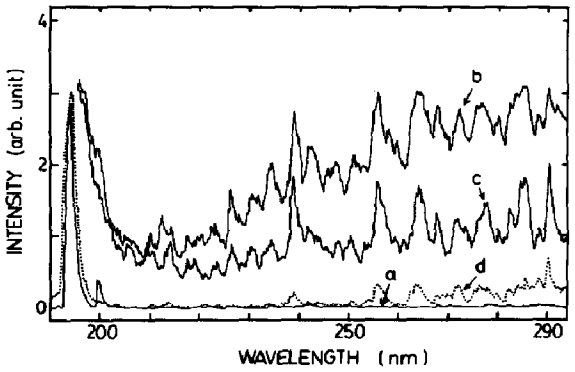

Fig. 2. Aerosol scattering and emission spectra produced from the ArF laser excitation (193 nm) of the O_3 and 1-C_4H_8 reaction products at various reaction distances (O_2 pressure, 114 Torr; O_3 pressure, 0.4 Torr; 1-C_4H_8 pressure, 0.2 Torr; monochromator resolution, 5 Å): spectrum a, 10 cm; spectrum b, 40 cm; spectrum c, 80 cm; spectrum d, 110 cm.

pulse^{-1} for spectrum a, 51 mJ pulse^{-1} for spectrum b, 46 mJ pulse^{-1} for spectrum c and 44 mJ pulse^{-1} for spectrum d.

When the reaction distance is 10 cm, only two bands have sufficient intensities as shown in Fig. 2, spectrum a. The band at 193 nm is the laser scattering light, and the other band at 199.5 nm is probably the Stokes shift of laser light by the gas. When the monochromator slit was widely open, additional bands from the $O_2(B^3\Sigma_u^-,\ v' = 4 \rightarrow X^3\Sigma_g^-,\ v'')$ system were observed. This O_2 emission has been recently reported by Shibuya and Stuhl [13]. Nevertheless, this emission is so weak that it does not appear in Fig. 2, spectrum a.

The rate constant for the O_3 and 1-C_4H_8 reaction is 1.23×10^{-17} cm^3 s^{-1} [14]. For a reaction distance of 10 cm, the reaction time is about 6 s, so about 60% of the 1-C_4H_8 molecules are consumed by O_3. O_3 attacks the double bond of 1-C_4H_8 to form primary ozonides which then develop to diradical intermediates. The diradical intermediates transform into small molecules, radicals or diradicals [6, 7]. The weak emission intensity shown in Fig. 2, spectrum a, indicates that the primary products of the O_3 and 1-C_4H_8 reaction in the gas phase do not emit when they are excited by ArF laser photons.

When the reaction distance increases to 40 cm, the laser scattering light at 193 nm increases greatly as shown in Fig. 2, spectrum b. This increase in scattering light indicates that aerosols or polymers are formed from the O_3 and 1-C_4H_8 reaction. As shown in Fig. 2, spectrum b, there are intense emission bands at wavelengths longer than the laser wavelength. It is noted that the emission bands have molecular structure.

The emission spectrum shown in Fig. 2, spectrum b, is very different from the emission spectrum produced by the ArF laser excitation of pure 1-C_4H_8 which is shown in Fig. 3. This spectrum was taken with a 1-C_4H_8 gas pressure of 1.2 Torr, a laser energy of 40 mJ pulse^{-1} and a monochromator resolution of 34 Å. The emission is presumably produced from two-photon

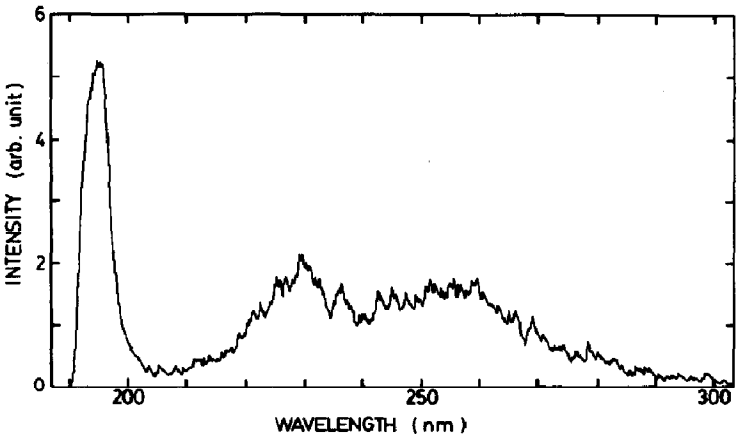

Fig. 3. The emission spectrum produced from the ArF laser excitation of pure 1-C_4H_8 (gas pressure, 1.2 Torr; laser energy, 40 mJ pulse^{-1}; monochromator resolution, 34 Å).

excitation. The emission intensity from the excitation of 1-C_4H_8 is so weak that it does not contribute significantly to the spectra shown in Fig. 2.

The emission intensity produced from the laser-induced chemical reactions in the gas cell is likely to be small and does not have a significant contribution to the emission signals observed. The most likely laser-induced reaction is initiated by O(^{1}D) produced from photodissociation of O_3. However, in the present experiment O(^{1}D) is most likely deactivated by O_2, because the [O_2] is much higher than the concentrations of other chemical species. In addition, as the excitation energy of O(^{1}D) is low (1.967 eV), it is unlikely that O(^{1}D) could produce energetic species emitting photons of energy higher than 5 eV as shown in Fig. 2, spectrum b. Furthermore, the amount of O_3 flowing to the gas cell is higher for the reaction distance of 10 cm (the case for Fig. 2, spectrum a) than that of 40 cm (the case for Fig. 2, spectrum b), so it is expected that the former case will produce more excited chemical species by laser-induced reactions than the latter case. However, this expectation is different from the observations shown in Fig. 2, spectra a and b. The emission intensity produced at the shorter reaction distance is smaller than that at the longer distance. Therefore, the emission observed in Fig. 2, spectrum b, is not caused by the laser-induced chemical reactions occurring in the gas cell; instead, it is likely to be caused by the laser excitation of products made in the flow tube.

Both the laser scattering light and the emission intensities vary greatly with the reaction distance. When the reaction distance increases to 80 cm, the emission intensity decreases as shown in Fig. 2, spectrum c. As the reaction distance further increases to 110 cm, the emission intensity decreases greatly as shown in Fig. 2, spectrum d. The laser scattering light intensity is also reduced to an amount similar to that for the reaction distance of 10 cm. This decrease suggests that the aerosols and/or polymers disappear when the reaction time is long. The aerosols and/or polymers may grow to large sizes as the reaction time increases and then deposit onto the wall of the flow

tube. Wei and Cvetanović [1] have observed that a non-volatile semitransparent liquid deposits onto the reaction vessel wall whenever O_3 reacts with olefins of more than four atoms.

The good correlation between the optical emission intensity and the laser scattering light intensity suggests that the optical emission at wavelengths longer than 200 nm is produced by a laser excitation of aerosols and/or polymers. More data for the good correlation between the emission and scattering intensities are shown in Section 3.2.1.

The emission spectrum produced by the excitation of aerosols with KrF laser photons (248 nm) is shown in Fig. 4. The spectrum was taken at $l = 40$ cm and O_3, 1-C_4H_8 and O_2 pressures of 0.1 Torr, 0.2 Torr and 120 Torr respectively. The monochromator resolution was set at 5 Å. The emission spectra taken at various O_3 and 1-C_4H_8 pressures are all very similar to the spectrum shown in Fig. 4.

The efficiency for the aerosol scattering is much larger than that for aerosol emission. There is a possibility that the observed emission bands (wavelengths longer than the laser wavelengths) may result from the aerosol scattering of the stray light inherent in the laser. To check this possibility, the laser light was reflected by mirrors before entering the gas cell. Each mirror is coated with a dielectric material so that it reflects only the laser wavelength. Thus, the stray light inherent in the laser is filtered out. The emission spectra taken with and without the mirror are the same. From these results it is concluded that the emission spectra are not produced by the aerosol scattering of laser stray light but by laser excitation of the aerosols.

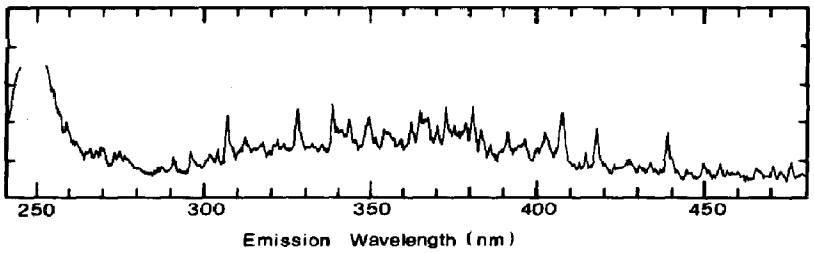

Fig. 4. Emission spectrum produced from the KrF laser excitation of aerosols produced at O_3, 1-C_4H_8 and O_2 pressures of 0.1 Torr, 0.2 Torr and 120 Torr respectively (reaction time, 24 *s*; reaction distance, 40 cm).

3.1.2. Excitation spectra

The above results clearly show that when aerosols are excited by the ArF and KrF laser photons they give scattering and emission light. The wavelength of the aerosol scattering light is the same as that of the light source, but the wavelength of the emission light is longer. The excitation spectra for producing both the aerosol scattering and the emission light were measured using UV light produced from various microwave discharge lamps. The results are shown in Fig. 5. The data were taken at an O_2 pressure of 107 Torr, a 1-C_4H_8 concentration of 3.3×10^{16} cm^{-3} and two O_3 concentrations

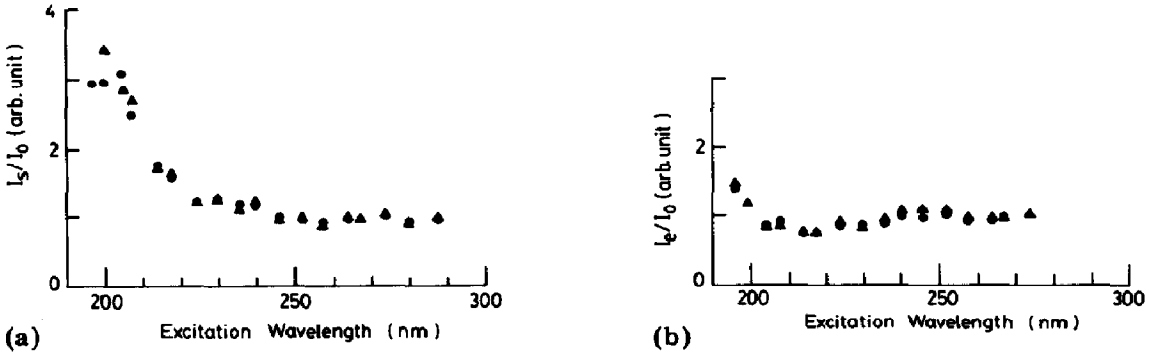

Fig. 5. (a) The ratio of scattering light intensity I_s to light source intensity I_0 at various excitation wavelengths without an optical filter (O_2 pressure, 107 Torr; [1-C_4H_8] = 3.3 × 10^{16} cm^{-3}; reaction distance, 40 cm) (the scattering light intensity was measured by a PMT with a response in the 180 - 800 nm region): ●, [O_3] = 8.5 × 10^{15} cm^{-3}; ▲, [O_3] = 3.7 × 10^{15} cm^{-3}. (b) The ratio of emission light intensity I_e to light source intensity I_0 at various excitation wavelengths. The aerosols were produced under the same conditions as in (a). The emission was measured by placing an optical filter ($\lambda > 300$ nm) in front of the PMT. The absolute emission signal is about 1% of the scattering signal.

of 3.7 × 10^{15} and 8.5 × 10^{15} cm^{-3}. The reaction distance was kept at 40 cm (reaction time, 24 s). The data are normalized to unity at the longest wavelengths measured. The scattering light was measured by a PMT (9558QB) with a response in the 180 - 800 nm region. The emission light of $\lambda > 300$ nm was measured by placing a long pass filter (Corning 0-54) in front of the PMT. Under the same experimental conditions, the emission intensity is only about 1% of the scattering intensity.

As shown in Fig. 5(a), the excitation function for the scattering intensity I_s to light source intensity I_0 ratio increases with decreasing excitation wavelength. This indicates that the aerosols have a greater concentration in the region of small size. The Rayleigh scattering intensity is proportional to a^6/λ^4, where a is the radius of an aerosol particle [15]. For effective scattering, the particle size parameter $2\pi a/\lambda$ will be close to unity [15]. For example, the aerosol particle radius will be near 0.03 μm if it is effectively scattered by a photon wavelength of 200 nm. Since the scattering light is more intense at 200 nm, as shown in Fig. 5(a), the aerosol particle sizes are probably in the region $a \approx 0.03$ μm. The particles of these sizes are called Aitken nuclei [16]. This particle size is comparable with the particle produced from the O_3 and isoprene reaction which is much smaller than 0.3 μm [4].

The excitation function for the emission intensity I_e to light source intensity I_0 ratio shown in Fig. 5(b) is different from the scattering excitation function. At the shorter excitation wavelengths, the emission intensity does not increase as much as the scattering intensity. The smaller increase in the emission intensity may be in part caused by the fact that the fraction of emission between the excitation wavelength and the filter cut-off (300 nm) is not included in the emission measurement. As shown in Figs. 2 and 4, the emission spectrum shifts to a short wavelength as the excitation wavelength

decreases. If we include the emission intensity for $\lambda < 300$ nm, the emission excitation function may be similar to that of the scattering excitation function. The emission intensity is thus closely correlated with the scattering intensity.

As shown in Fig. 5, both the scattering and the emission excitation functions do not vary with $[O_3]$, which changes from 3.7×10^{15} to 8.5×10^{15} cm^{-3}. These results indicate that the aerosol particle sizes and the chemical species are similar, even though they are formed by different aerosol formation processes. The dependence of aerosol formation on $[O_3]$ is described below.

3.2. Aerosol formation process

3.2.1. $[O_3]$ dependence

The scattering and emission intensities at various $[O_3]$ are shown in Fig. 6. The excitation light source wavelength is 206 nm which is produced from a microwave discharge iodine lamp and isolated by a 0.25 m monochromator. The O_2 pressure is 120 Torr and $[1\text{-}C_4H_8] = 2 \times 10^{16}$ cm^{-3}. The reaction distance is fixed at 40 cm. The scattering light at 206 nm is isolated by a 0.5 m monochromator. The emission light is observed by a combination of a PMT and an optical long pass filter whose total combination response is in the 300 - 800 nm region. Both the scattering and the emission intensities are normalized to an equal value at the highest $[O_3]$ measured. As stated before, the emission intensity is only about 1% of the scattering intensity.

At low $[O_3]$, both the scattering and the emission intensities shown in Fig. 6 increase as $[O_3]^{2.2}$. As the $[O_3]$ increases, the scattering and emission

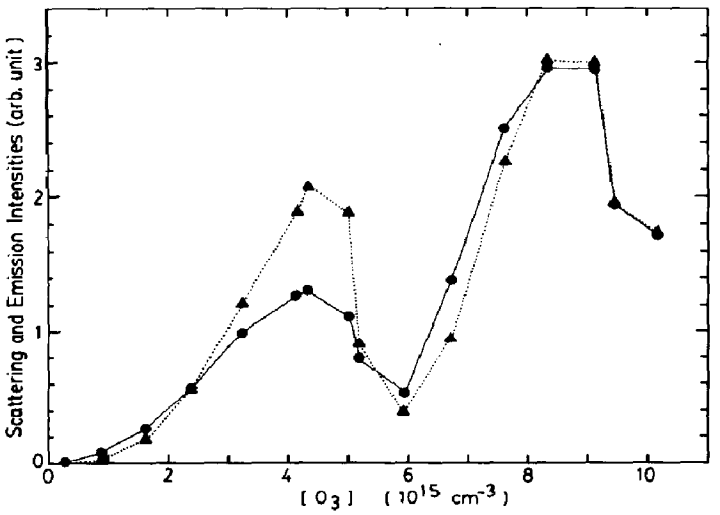

Fig. 6. The dependence of aerosol scattering and emission intensities on $[O_3]$ (excitation wavelength, 206 nm; O_2 pressure, 120 Torr; $[1\text{-}C_4H_8] = 2 \times 10^{16}$ cm^{-3}; reaction distance, 40 cm): ●, scattering light isolated by a monochromator at 206 nm; ▲, emission light measured at wavelengths longer than 300 nm. The scattering and emission light are normalized at the highest $[O_3]$ measured.

intensities increase and reach a maximum at $[O_3] = 4.3 \times 10^{15}$ cm^{-3}; the intensities then decrease very quickly with increasing $[O_3]$. When $[O_3]$ is higher than 6×10^{15} cm^{-3}, the intensities increase again and reach a second maximum at $[O_3] = 8.3 \times 10^{15}$ cm^{-3}. The intensities decrease at high $[O_3]$.

The data shown in Fig. 6 suggest that the aerosol formation processes at low $[O_3]$ are different from the process at high $[O_3]$. At low $[O_3]$, aerosol formation is likely to start with active chemical radicals that are initially produced from the molozonides. The radical concentration initially produced by the O_3 and 1-C_4H_8 reaction is expected to increase with $[O_3]$, so the aerosol concentration will increase with $[O_3]$. When the number and size of aerosol particles increase, the particles will coagulate. The larger are the number and size of aerosol particles, the higher the coagulation rate is [15]. Thus, the number of aerosol particles will decrease at high $[O_3]$. The first aerosol peak shown in Fig. 6 may result from these processes. The molozonides may also develop into some chemical species that will produce an aerosol with a slower rate than the active species. In addition, some radicals that are later produced by secondary chemical reactions may also eventually evolve into aerosols. These slow aerosol formation processes will need greater radical concentrations to make embryos, so they require a greater $[O_3]$. These slow processes may be responsible for the second aerosol peak at high $[O_3]$ as shown in Fig. 6.

The dependence of emission intensity on $[O_3]$ is very similar to that of scattering intensity as shown in Fig. 6. The similarity of these two intensities is also observed in other measurements such as when the [1-C_4H_8] and the reaction time are varied. The correlation between the emission and scattering intensities is shown in Fig. 7, in which the data were taken at various gas concentrations and reaction distances. The emission intensity is linearly dependent on the scattering intensity within the statistical uncertainty. The

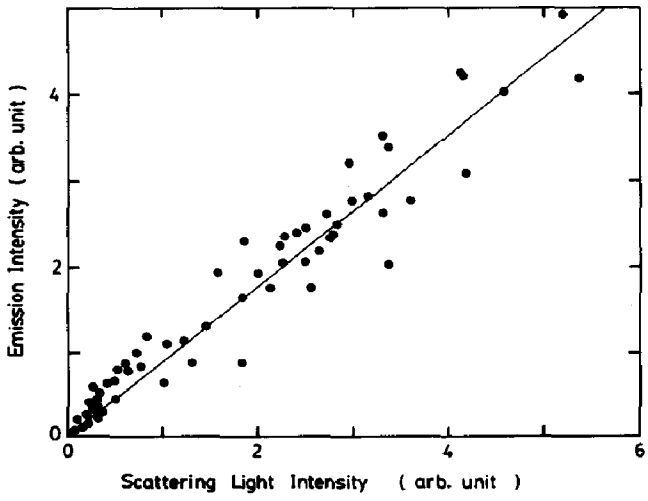

Fig. 7. The correlation between the emission and scattering light intensities. The data were taken at various $[O_3]$, [1-C_4H_8] and reaction distances.

close correlation between the emission and scattering intensities again indicates that the emission is produced from the UV excitation of aerosols. Because of this similarity, we shall present only the scattering intensity data in the following sections.

The scattering intensity is greatly affected by the [1-C_4H_8] as shown in Fig. 8 for the scattering light intensity *versus* [O_3]. The data were taken under conditions similar to those in Fig. 6, except for the change in [1-C_4H_8] to 0.5×10^{16}, 1.3×10^{16} and 5×10^{16} cm^{-3}. For [1-C_4H_8] = 5×10^{15} cm^{-3}, the scattering intensity has a maximum at [O_3] $\approx 3 \times 10^{15}$ cm^{-3}. At this [O_3], the 1-C_4H_8 may be totally consumed by O_3. At this maximum, the ratio [1-C_4H_8]/[O_3] = 1.7, which is consistent with the observation of Wei and Cvetanović [1] that every O_3 molecule will consume 1.4 - 2.0 olefin molecules in O_2. The scattering intensity decreases at high [O_3], which may be in part caused by O_3 reaction with aerosol precursors and/or by O_3 destruction of aerosols. This decrease may be also partly caused by the decrease in the light source intensity in the PMT viewing region by O_3 absorption.

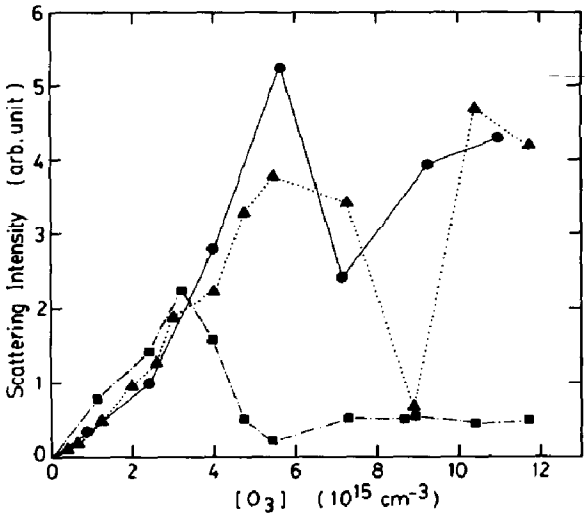

Fig. 8. The dependence of aerosol scattering light intensity on [O_3] for various [1-C_4H_8] (the excitation wavelength, the O_2 pressure and the reaction distance are the same as in Fig. 6): ■, [1-C_4H_8] = 0.5×10^{16} cm^{-3}; ●, [1-C_4H_8] = 1.3×10^{16} cm^{-3}; ▲, [1-C_4H_8] = 5×10^{16} cm^{-3}.

Taking the reaction rate constant as 1.23×10^{-17} cm^3 s^{-1} [14], the [O_3] will decrease to e^{-1} within 16 s, if [O_3] < [1-C_4H_8]. For a reaction distance of 40 cm used here, the reaction time is 24 s. Thus, most of the O_3 molecules will be consumed by 1-C_4H_8 before they reach the optical excitation region. When the initial [O_3] becomes larger than the initial [1-C_4H_8], 1-C_4H_8 molecules will be consumed by O_3 before they reach the gas cell. Once the 1-C_4H_8 molecules are consumed out, the probability for developing the reaction products into aerosols becomes small. This is another reason

explaining the scattering intensity decrease at high $[O_3]$ for $[1\text{-}C_4H_8] = 5 \times 10^{15}$ cm^{-3} as shown in Fig. 8.

When the $[1\text{-}C_4H_8]$ increases to 1.3×10^{16} and 5×10^{16} cm^{-3}, the intensities have a maximum at $[O_3] \approx 5.5 \times 10^{15}$ cm^{-3}. At low $[O_3]$, the scattering intensity does not vary significantly with the change in $[1\text{-}C_4H_8]$. This indicates that the aerosol formation is mainly determined by the initial $[O_3]$. In other words, the aerosol concentration is mainly determined by the concentration of the active species initially produced by the O_3 and $1\text{-}C_4H_8$ reaction. As the $[O_3]$ increases, the scattering light intensity increases again at high $[1\text{-}C_4H_8]$. This increase may be a result of the less active species and/or the secondary reactions that require high $[O_3]$ and $[1\text{-}C_4H_8]$ to grow into aerosols. This description is consistent with the two-process aerosol formation model, which can also be used to describe other data below.

3.2.2. $[1\text{-}C_4H_8]$ *dependence*

The dependence of scattering intensity on the $[1\text{-}C_4H_8]$ is shown in Fig. 9. The aerosols are excited by the iodine resonance lamp at 206 nm. The O_2 pressure is 120 Torr and the O_3 concentrations are 3.6×10^{15}, 7.0×10^{15} and 10×10^{15} cm^{-3}. The reaction distance is fixed at 40 cm.

At $[O_3] = 3.6 \times 10^{15}$ cm^{-3}, the scattering intensity builds up slowly with increasing $[1\text{-}C_4H_8]$ up to 7×10^{15} cm^{-3}, where O_3 is totally consumed. The $[O_3]$ will decrease to e^{-1} within 10 s for $[1\text{-}C_4H_8] > 7 \times 10^{15}$ cm^{-3}, if we take the reaction rate constant to be 1.23×10^{-17} cm^3 s^{-1} [14]. For a reaction time of 24 s, the O_3 molecules will be mostly consumed before they reach the gas cell. When the $[1\text{-}C_4H_8]$ is larger than 7×10^{15} cm^{-3}, the aerosols are formed earlier and lost before they reach the gas cell, so the intensity decreases at high $[1\text{-}C_4H_8]$. As the $[1\text{-}C_4H_8]$ increases, the scattering intensity shows a second maximum at $[1\text{-}C_4H_8] = 2.5 \times 10^{16}$ cm^{-3}. This

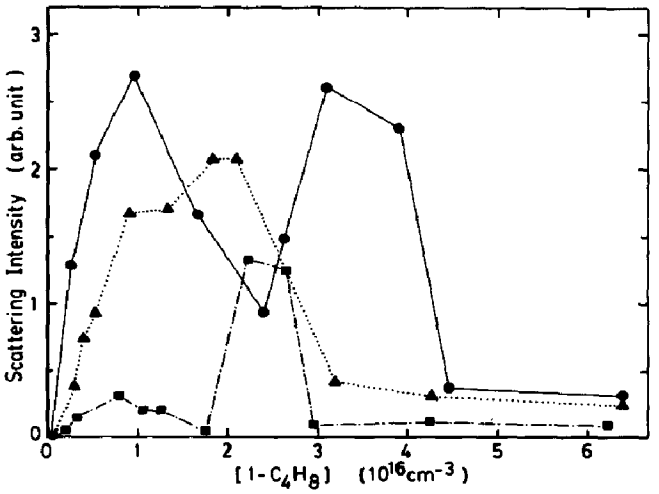

Fig. 9. The dependence of aerosol scattering light intensity on $[1\text{-}C_4H_8]$ for various $[O_3]$ (the excitation wavelength, the O_2 pressure and the reaction distance are the same as in Fig. 6): ■, $[O_3] = 3.6 \times 10^{15}$ cm^{-3}; ▲, $[O_3] = 7.0 \times 10^{15}$ cm^{-3}; ●, $[O_3] = 10 \times 10^{15}$ cm^{-3}.

second maximum may be made by the less active species and/or the second products that require a higher [1-C_4H_8] to form aerosols. Again, these results of two maxima indicate that the aerosols are produced by two different formation processes.

When the [O_3] increases, the scattering light intensity increases more rapidly at low [1-C_4H_8]. The aerosols may be formed by combining several embryos, so the higher the number of active chemical species, the quicker the aerosols are formed. At low [1-C_4H_8], the scattering intensity increases with increasing [O_3] as shown in Fig. 9. This increase indicates that the aerosol concentration is determined by the active species (produced by the O_3 and 1-C_4H_8 reaction) whose concentration is determined by the initial [O_3].

When the [O_3] increases to 10^{16} cm^{-3}, the scattering intensity increases steeply at low [1-C_4H_8] and reaches a maximum at [1-C_4H_8] = 10^{16} cm^{-3}. The scattering intensity exhibits a second peak at high [1-C_4H_8]. These double maxima again illustrate the two-process aerosol formation model. The formation of aerosol at the second peak may require a large amount of radicals because of its slow formation rate.

3.2.3. Reaction time dependence

The dependence of aerosol scattering intensity on the reaction distance is shown in Fig. 10. The reaction distance can be converted into reaction time by dividing it by the flow velocity of 1.7 cm s^{-1}. The light source is the iodine resonance lamp (206 nm). The data were taken at an O_2 pressure of 120 Torr, a 1-C_4H_8 concentration of 1.3×10^{16} cm^{-3} and O_3 concentrations of 10^{15}, 3.6×10^{15} and 1.2×10^{16} cm^{-3}.

When [O_3] = 10^{15} cm^{-3}, it takes a reaction distance of 50 cm (reaction time, 30 s) to produce the maximum aerosol concentration, and the aerosol concentration decreases quickly at longer reaction distance as shown in

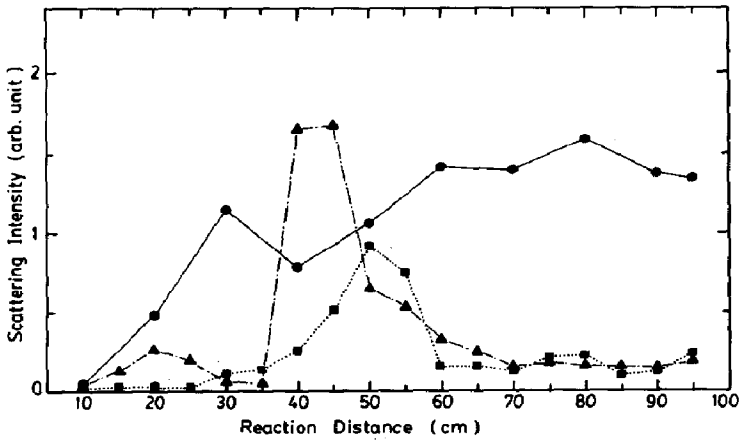

Fig. 10. The dependence of aerosol scattering light intensity on reaction distance at various [O_3] (excitation wavelength, 206 nm; O_2 pressure, 120 Torr; [1-C_4H_8] = 1.3×10^{16} cm^{-3}): ■, [O_3] = 10^{15} cm^{-3}; ▲, [O_3] = 3.6×10^{15} cm^{-3}; ●, [O_3] = 12×10^{15} cm^{-3}.

Fig. 10. The rate constant for O_3 and 1-C_4H_8 is 1.23×10^{-17} cm^3 s^{-1} [14]. Thus, O_3 will be consumed by 1-C_4H_8 to the value e^{-1} within 10 cm. However, at this reaction distance the aerosol concentration is very small. It takes a much longer time to build up aerosols. When the [O_3] increases, the build-up time for aerosol formation decreases. These results again suggest that aerosols are formed by a combination of several embryos which are originally from the O_3 and 1-C_4H_8 reaction products. The higher the [O_3], the greater the amount of reaction products there will be. Thus, the aerosol build-up time will be shorter at high [O_3]. This is consistent with the previous interpretation for the dependence of aerosol scattering intensity on [O_3] and [1-C_4H_8].

For [O_3] = 1×10^{15} cm^{-3} and [O_3] = 3.6×10^{15} cm^{-3}, the aerosol concentrations decrease quickly at high reaction distance, and they do not increase again at the longer reaction distance. However, when [O_3] increases to 1.2×10^{16} cm^{-3}, the scattering light increases again at longer reaction distance. This increase is probably caused by the slow aerosol formation processes which may be initiated by the less active chemical species and/or the secondary reaction products. The two-process aerosol formation model is again supported by this result.

4. Concluding remarks

The experimental results seem to point to a conclusion that the aerosols are produced from two different formation processes. The first scattering intensity peak shown at low [O_3], low [1-C_4H_8] or short reaction time probably resulted from the active chemical species initially produced from the O_3 and 1-C_4H_8 reaction. At high [O_3], high [1-C_4H_8] and long reaction time, the less active chemical species and/or the secondary products may be present in sufficient concentration to produce a second maximum. However, the ozonolysis process of 1-C_4H_8 is very complicated. To identify the chemical species responsible for the aerosol formation is not a simple task.

It is suggested that O_3 initially attacks the double bond of 1-C_4H_8 to form molozonides [6, 7], which then split into small molecules and radicals by the Criegee mechanism [6] and by hydrogen atom abstraction [7]. O'Neal and Blumstein [7] estimated that the hydrogen atom abstraction had higher rates than the rate of the Criegee split. However, Niki *et al.* [17] later showed that the Criegee mechanism was also important in the gas phase ozonolysis of *cis*-2-butene. The fast aerosol formation process may result from the peroxy radicals (formed in the Criegee split and the hydrogen atom abstraction) which are active chemical species. They will transform into other products and may eventually evolve into aerosols by further reactions with 1-C_4H_8.

The current results demonstrate that optical excitation is a useful technique for studying aerosol formation processes. However, for a further detailed understanding of aerosol formation processes, the reaction products

produced from either primary ozonolysis or a secondary reaction process are needed. The particle size distribution and the chemical composition of aerosols are also needed for studying the aerosol formation kinetics.

Molecular structure always appears in the emission spectra in spite of aerosols formed at various $[O_3]$, $[1\text{-}C_4H_8]$ and reaction times. The structures shown in the emission spectra produced by the ArF and KrF laser excitation of aerosols have similar characteristics. The cause of the observed emission is not clear at this moment and will be pursued further in this research program.

Acknowledgments

We wish to thank Dr. H. Akimoto at the National Institute for Environmental Studies, Japan, Professor O'Neal, Dr. F. Li and Dr. J. B. Nee at San Diego State University for useful discussions and Mr. J. S. Lai for technical assistance. This material is based on the work supported by the National Science Foundation under Grant ATM-8203948.

References

1 Y. K. Wei and R. J. Cvetanović, *Can. J. Chem., 41* (1963) 397.
2 W. B. DeMore, *Int. J. Chem. Kinet., 1* (1969) 209.
3 L. A. Ripperton, H. E. Jeffries and O. White, *Adv. Chem. Ser., 113* (1972) 219.
4 R. M. Kamens, M. W. Gery, H. E. Jeffries, M. Jackson and E. I. Cole, *Int. J. Chem. Kinet., 14* (1982) 955.
5 R. L. Day and L. C. Lee, *Appl. Opt., 22* (1983) 2546.
6 P. S. Bailey, *Ozonation in Organic Chemistry*, Academic Press, New York, 1978.
7 H. E. O'Neal and C. Blumstein, *Int. J. Chem. Kinet., 5* (1973) 397.
8 P. A. Leighton, *Photochemistry of Air Pollution*, Academic Press, New York, 1961.
R. F. Gould (ed.), *Photochemical Smog and Ozone Reactions, Adv. Chem. Ser., 113* (1972).
G. M. Hidy, P. K. Mueller, D. Grosjean, B. R. Appel and J. J. Wesolowski (eds.), *The Character and Origins of Smog Aerosols*, Wiley, New York, 1980.
9 A. P. Altshuller and J. J. Bufalini, *Environ. Sci. Technol., 5* (1971) 39.
10 H. Niki, E. E. Daby and B. Weinstock, *Adv. Chem. Ser., 113* (1972) 16.
11 J. A. R. Samson, *Techniques of Vacuum Ultraviolet Spectroscopy*, Wiley, New York, 1967.
12 W. Slavin, R. W. Mooney and D. T. Palumbo, *J. Opt. Soc. Am., 51* (1961) 93.
13 K. Shibuya and F. Stuhl, *J. Chem. Phys., 76* (1982) 1184.
14 S. M. Japar, C. H. Wu and H. Niki, *J. Phys. Chem., 78* (1974) 2318.
15 S. Twomey, *Atmospheric Aerosols*, Elsevier, Amsterdam, 1977.
16 C. E. Junge, *Air Chemistry and Radioactivity*, Academic Press, New York, 1963.
17 H. Niki, P. D. Maker, C. M. Savage and L. P. Breitenbach, *Chem. Phys. Lett., 46* (1977) 327.